Supplementary information for: Charge transport in a quantum dot supercrystal

Iek-Heng Chu[(1)], Marina Radulaski[(2,4)], Nenad Vukmirovic[(3,4)], Hai-Ping Cheng[(1)], Lin-Wang Wang[(4)]

(1) Department of Physics and Quantum Theory Project, University of Florida, Gainesville, FL 32611

(2) Faculty of Physics, University of Belgrade, Studentski trg 12-15, 11000 Belgrade, Serbia

(3) Scientific Computing Laboratory, Institute of Physics Belgrade, University of Belgrade, Pregrevica 118, 11080 Belgrade, Serbia

(4) Material Science Division, Lawrence Berkeley National Laboratory, One Cyclotron Road, Mail Stop 66, Berkeley, CA 94720

Email: lwwang@lbl.gov

(1) The smooth cut-off of the charge density and the patch up of the three pieces in Figure 2:

The charge densities in the quantum dot part (both the left and right pieces) as well as the molecule part (the central piece), as illustrated in Figure 2, are computed individually. To patch them up for the total charge density, a mask function $w(\vec{r})$ is introduced which varies smoothly from 0 to 1 when $\vec{r}$ crosses the dashed line in Figure 2 from the quantum dot side to the central molecule side. More specifically, $w(\vec{r}) = 1/(e^{a(d-b)}+1)$, otherwise $w(\vec{r})$ is 0 in the quantum dot part and 1 in the molecule part. Here, $d = |\vec{r} - \vec{r}_{dash}|$ is the shortest distance between $\vec{r}$ and the red dashed line. In the calculations, *a* and *b* are taken as 12.8Å^{-1} and 0.469Å, respectively. The result is insensitive to the exact values of a and b. The total charge density is then calculated as $\rho(\vec{r}) = w(\vec{r})\rho_{center}(\vec{r}) + (1 - w(\vec{r}))\rho_{QD}(\vec{r})$. It is worth mentioning that in order to yield the correct total charge, one might need to rescale the center charge density $\rho_{center}(\vec{r})$ very slightly.

(2) The details of the surface molecule attachment calculations:

The attachment between the molecule Sn_2S_6 and a flat CdSe (1010) surface is modeled by a three-layer slab adsorbed with the molecules. An orthorhombic supercell with dimension of 14.69 x 12.72 x 33.03 $Å^3$ is used in the calculations, in which the slab is periodic in the *x*-*y* plane with a 10 Å vacuum region along the *z* direction. The separation between the neighboring molecules is 10 Å so that the interactions between the molecules can be neglected. The total energy minimizations were performed using density functional theory (DFT)[1, 2] in local density approximation[3], as implemented in the plane-wave based VASP code[4, 5]. Ultrasoft pseudopotentials[6] with a kinetic energy cutoff of 400eV were used to ensure the total energy convergence. Several initial molecule attachment configurations are tested, followed by atomic relaxations. The two lowest energy attachments after the atomic relaxations are shown in Figure 3.

(3) Electron-phonon coupling:

The electron-phonon coupling is calculated by the charge patching method. There are two terms in the single particle Hamiltonian derivative $\partial H / \partial \vec{R}$. The first term is the change of the nonlocal potential in Eq.(1), which is calculated using the conventional method as in a total energy plane wave code. The second term is the change of the local potential, especially the Hartree potential. This is due to two parts; one is the displacement of the nuclei charge, which is represented by the local part of the pseudopotential. Another part is due to the change of valence electron charge density, and consequently the change of the Hartree potential. We have used the CPM[7] to calculate the change of the charge density when an atom is moved. Note, only the charge motifs near the atom $\vec{R}$ need to be changed. This makes the method extremely efficient. This method has been used to calculate the electron-phonon coupling in organic polymer systems[8-10]. Here, in inorganic nanocrystals, we found that it is necessary to screen the long range part of the potential change $\Delta V(\vec{r})$ due to the atomic displacement at $\vec{R}$. This is because, in CPM, the charge density is not calculated self-consistently; as a result, the long range electric field is not screened. We have thus multiplied a fixed spherical screening function $f(|\vec{r}-\vec{R}|)$ on top of $\Delta V(\vec{r})$ (caused by a single atom displacement at $\vec{R}$), here $f(x)$ is a function which is close to 1 when *x* is near zero, and roughly 1/ε when *x* is large, and ε is

the bulk dielectric constant. In practice, the $f(x)$'s for Cd displacement and Se displacement are also different. We obtain this mask function from bulk system calculations where direct DFT calculations have been carried out. $f(x)$ is computed as the ratio of the $\Delta V(\vec{r})$ obtained from CPM and DFT methods. We then use this mask function in the calculation of quantum dot systems.

After $f(x)$ is multiplied to the local potential change $\Delta V(\vec{r})$, we can now calculate the electron-phonon coupling constants: $C_{i,j}(\vec{R}) = \langle \psi_i | \partial H / \partial \vec{R} | \psi_j \rangle$. The results are shown in Figure S1 for the smallest quantum dot where the $\partial H / \partial \vec{R}$ can also be calculated directly from self-consistent DFT calculations. About 20 *i* and *j* are used. One can see that the overall CPM error is probably about 30% especially when the largest electron-phonon couplings are considered. Furthermore, there is no systematic error.

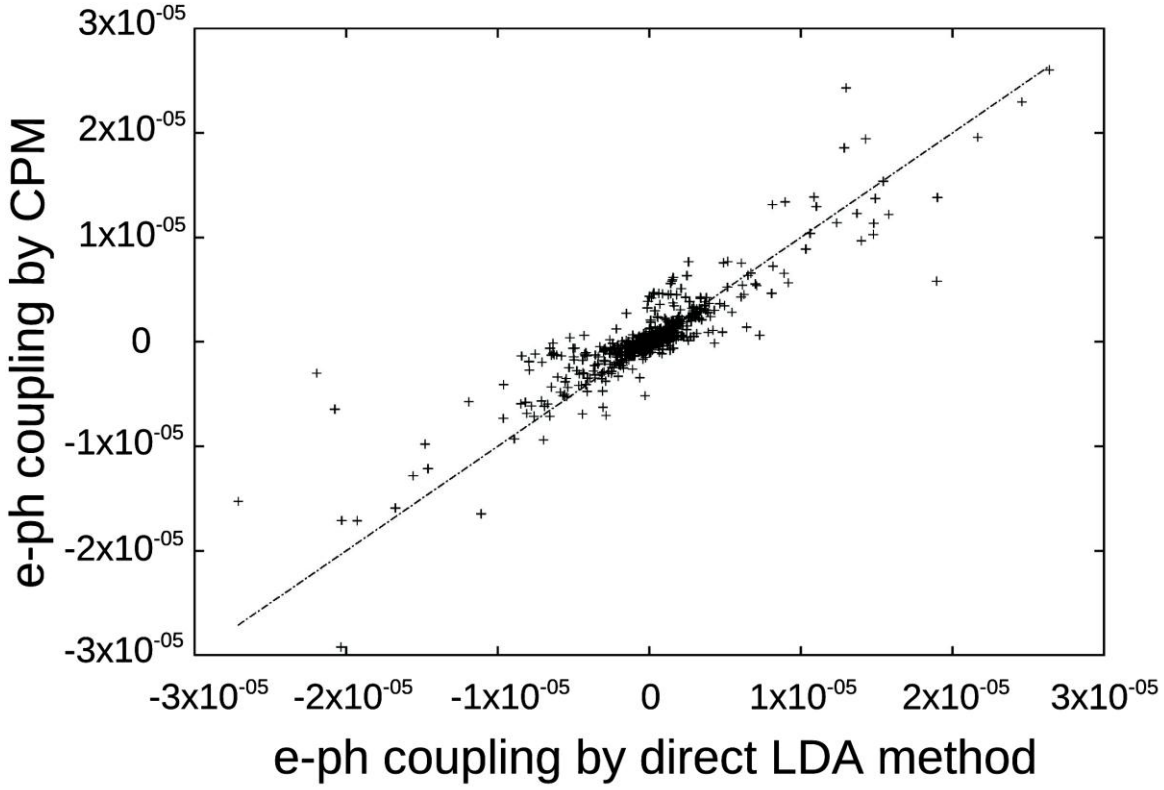

Figure S1: A comparison between the calculated electron-phonon couplings (in a.u.) for a few atomic displacements (near the center and near the surface) from the CPM and the direct DFT-LDA calculations.

(4) The quantum dot size scaling of the reorganization energy λ:

The calculated λ is plotted as a function of the inverse of the total number of atoms N in Figure S2. A straight line relationship is observed. Such scaling feature can be understood as the following. For each atomic movement, the electron-phonon coupling constant scales as $1/\Omega$, where Ω is the volume of the quantum dot. This is due to the normalization of the wave function ψ_i. For a harmonic oscillator with a spring constant of k, if an external force $C_{i,i}(\vec{R})$ is applied to this oscillator, the relaxation energy (reorganization energy) will be $-0.5C_{i,i}^2(\vec{R})/k \propto 1/\Omega^2$. Since the number of atoms is also proportional to Ω, the overall reorganization energy λ is proportional to $1/\Omega$.

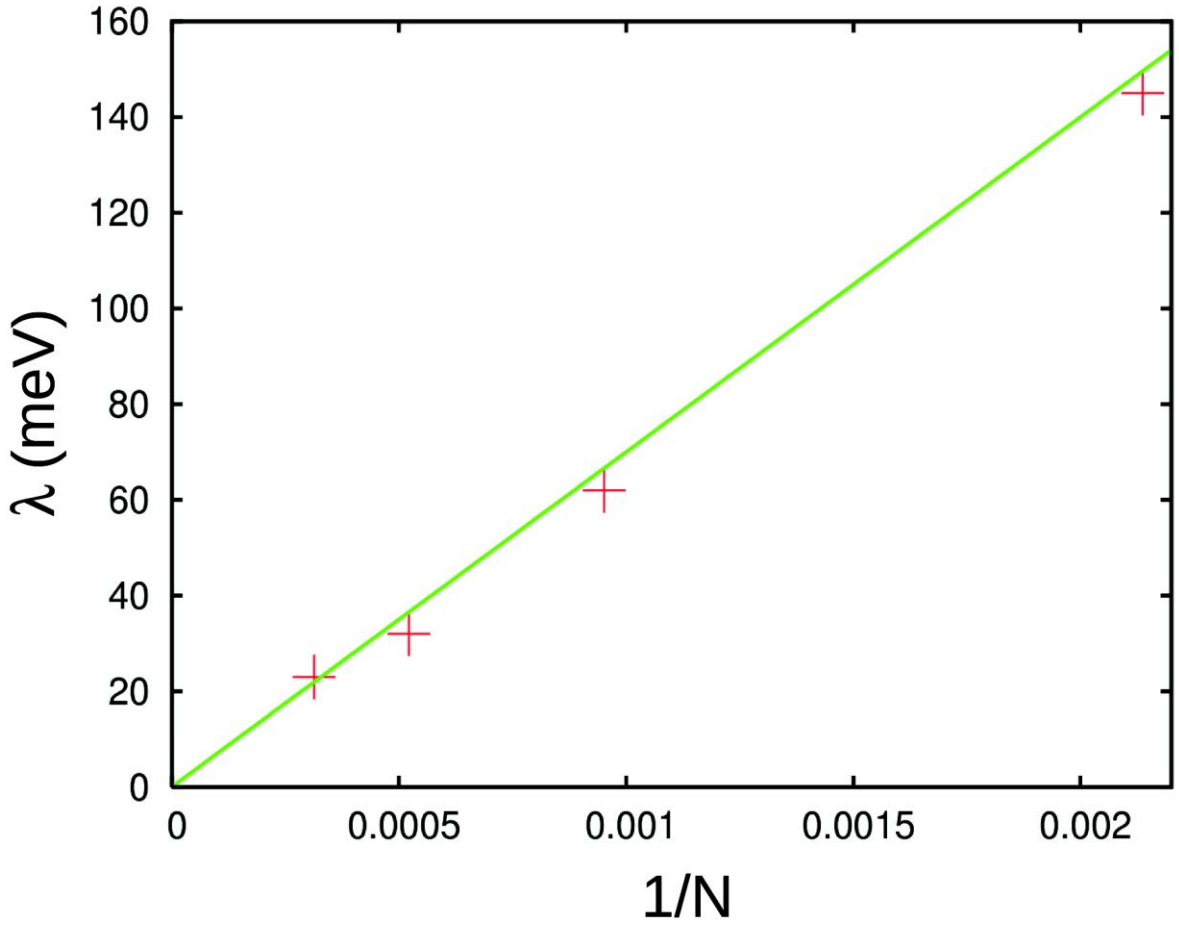

Figure S2: The calculated reorganization energies λ as a function of the inverse of the number of atoms ($1/N$). The green line indicates a linear fit.

(5) Local density of state calculations:

The generalized moment method (GMM)[11] is used to calculate the local density of states (LDOS) at the molecule Sn_2S_6. The results are shown in Figure S3, Figure S4 for the two different attachments, respectively. From the LDOS, one can see where the local states start to appear. Comparing that to the QD conduction band minimum (CBM), we can get the barrier height ΔE as shown in Figure 1(C). We found that such ΔE is about 2.4 eV for the large QDs. For the smaller QDs, this barrier height drops to ~1.8 eV due to quantum confinement effect of the CBM.

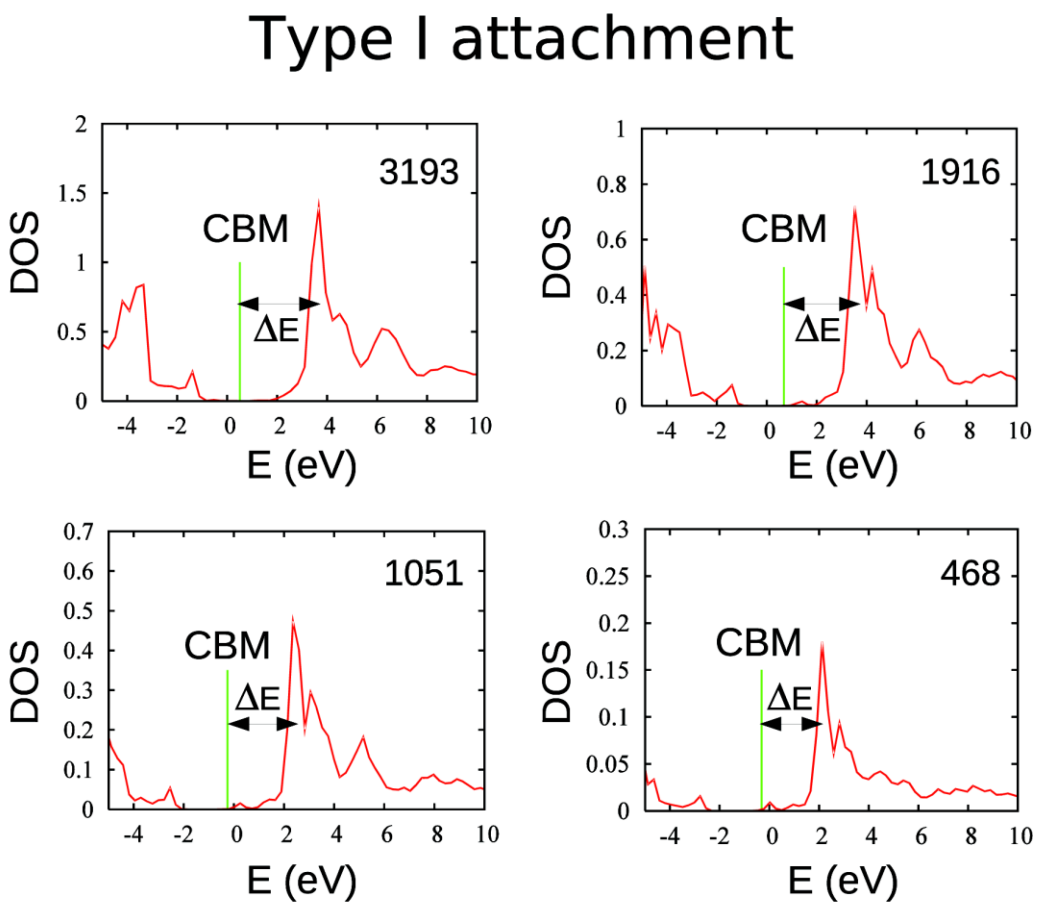

Figure S3: The local density of states at the molecule site for type I attachment. The eigen-energies of CBM for different QD sizes (the number of atoms is indicated in the top right corner of each panel) are shown by the green vertical lines. ΔE is the estimated barrier height in the over-the-barrier activation mechanism.

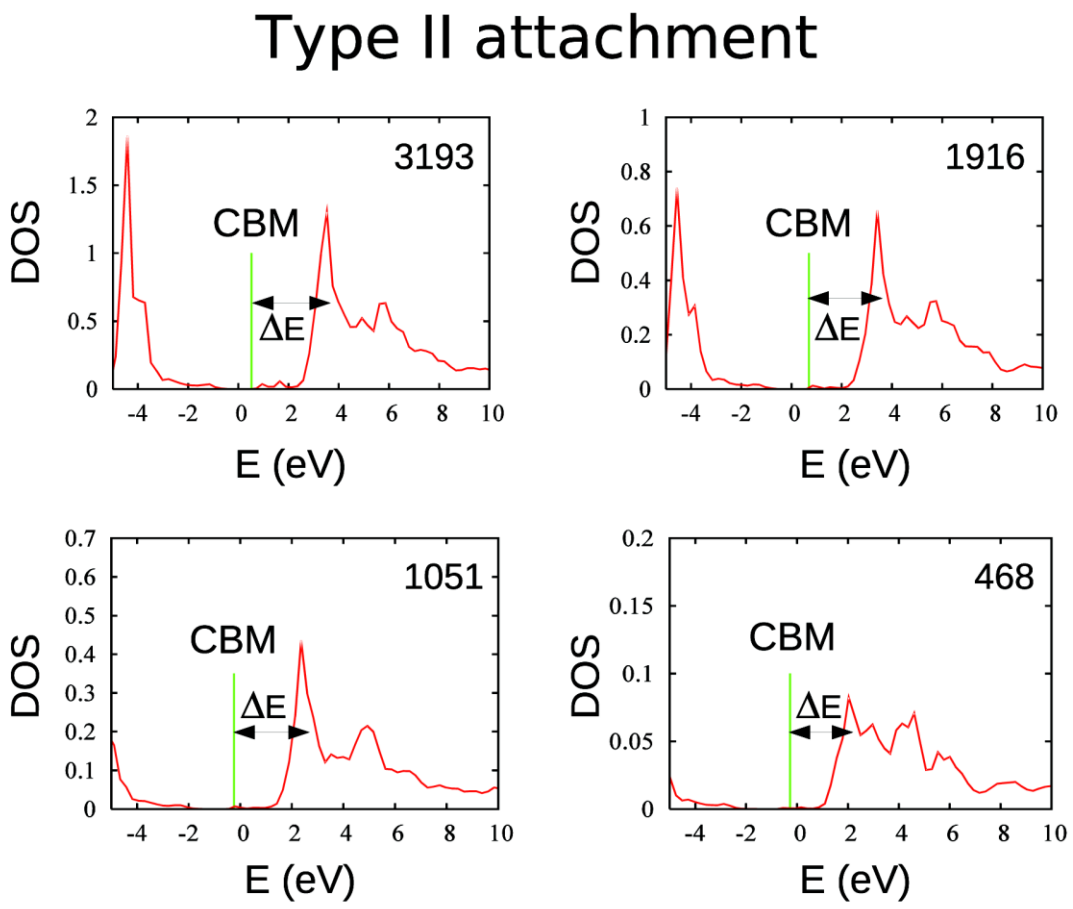

Figure S4: The local density of states at the molecule site for type II attachment. All the notations are the same as in Figure S3.

(6) Mobility calculation for the supercrystal:

With hopping rates between quantum dots at hand, one can calculate the electron mobility at low carrier density and low electric fields using the following procedure. Let τ_{ab}^{-1} be the hopping rate between two quantum dots *a* and *b*. It is known[12] that the electrical transport at low electric field and low carrier density is fully equivalent to the transport in a network of conductors where any two neighboring quantum dots have been connected with a conductance $G_{ab} = G_{ba} = e^2 n_a \tau_{ab}^{-1} / k_B T = e^2 n_b \tau_{ba}^{-1} / k_B T$ where n_a is the equilibrium occupation of state *a* given by the Boltzmann distribution, *e* is the elementary charge and k_B is the Boltzmann constant.

We construct the portion of the cubic supercrystal with $n_1 \times n_2 \times n_3$ quantum dots (of the size $L_x = L_y = L_z = L$), where $n_1 = n_2 = n_3 = 50$, i.e. a conductor network of the same dimensions. The equivalent conductance of such network is found by solving the linear equations for the potential of nodes in the circuit. These equations read $\sum_j (V_i - V_j) G_{ij} = 0$ where *j* is a neighbor of *i*. Periodic boundary conditions for V_i are applied in two directions (say *y* and *z*). For the *x* direction, we have $V_i = 0$ for the first *y*-*z* plane, and $V_i = U$ for the n_1-th *y*-*z* plane. A linear equation is then formed to solve for V_i in the interior planes. The current I_x through a plane perpendicular to the *x* direction is then calculated and the equivalent conductance is found as $G_x = I_x / U$. The mobility in *x*-direction is then given by $\mu_x = G_x / neL$, where *n* is the average concentration of carriers. Using the size fluctuation, we have randomly assigned the size, hence ε_i on each QD according to the fluctuation. We have calculated the G_{ab} using Eq.(2). To simulate the effects of loose attachment we have also multiplied G_{ab} with a random number uniformly distributed among 0 and 1.

References

1. Hohenberg, P.; Kohn, W. *Phys. Rev. B* **1964,** 136, (3B), B864.
2. Kohn, W.; Sham, L. J. *Phys. Rev.* **1965,** 140, (4A), 1133.
3. Perdew, J. P.; Zunger, A. *Phys. Rev. B* **1981,** 23, (10), 5048-5079.
4. Hafner, G. K. a. J. *Phys. Rev. B* **1993,** 47, (1), 558–561.
5. Kresse, G.; Furthmuller, J. *Phys. Rev. B* **1996,** 54, (16), 11169-11186.
6. Vanderbilt, D. *Phys. Rev. B* **1990,** 41, (11), 7892-7895.
7. Wang, L. W. *Phys. Rev. B* **2002,** 65, (15), 153410.
8. Vukmirovic, N.; Wang, L. W. *Nano Lett.* **2009,** 9, (12), 3996-4000.
9. Vukmirovic, N.; Wang, L. W. *Appl. Phys. Lett.* **2010,** 97, (4), 043305.
10. Vukmirovic, N.; Wang, L. W. *Phys. Rev. B* **2010,** 81, (3), 035210.
11. Wang, L. W. *Phys. Rev. B* **1994,** 49, (15), 10154-10158.
12. Ambegaokar, V.; Halperin, B. I.; Langer, J. S. *Phys. Rev. B* **1971,** 4, (8), 2612-2620.